Journal of Power Sources 193 (2009) 107–115

Contents lists available at ScienceDirect

Journal of Power Sources

journal homepage: www.elsevier.com/locate/jpowsour

Experimental investigation of parameters influencing the freeze start ability of a fuel cell system

Eva Schießwohl[a,*], Thomas von Unwerth[a], Frank Seyfried[a], Dieter Brüggemann[b]

[a] Volkswagen AG, Letter Box 1172, D-38436 Wolfsburg, Germany
[b] Lehrstuhl für Technische Thermodynamik und Transportprozesse, Universität Bayreuth, Germany

ARTICLE INFO

Article history:
Received 2 October 2008
Received in revised form 11 November 2008
Accepted 22 November 2008
Available online 7 December 2008

Keywords:
Fuel cell system
Freeze start

ABSTRACT

To improve the freeze start ability of a fuel cell system some significant influencing parameters are defined and investigated. Experiments with a fuel cell test system are carried out in a climate chamber at various conditions. The time interval until fuel cell stack power equals 50% of its maximum power is defined as an indicator for a successful freeze start as well as a value for comparison and evaluation of the results. The target of this work is the minimization of this freeze start time by avoiding the freezing of process water on the catalyst layer of the Membrane Electrode Assembly (MEA), since this leads to temporary performance losses.

The shut down strategy of the fuel cell system is identified to be one of the main parameters influencing the freeze start. It is found that a higher degree of dryness in the stack leads to a significant improvement in the freeze start performance, since the water absorbing capacity of the membrane increases and therefore also the time until its saturation. If this saturation takes place after the temperature of the MEA reached 0 °C, no significant ice-formation occurs. It is shown that by improving the shut down strategy of the fuel cell system at $T_{Start} = -6$ °C a start without performance loss can be realized. At temperatures lower than that temporary performance losses occur.

Even if a lower voltage leads to a higher current and therefore to a higher water production rate, its effect on the freeze start due to the increased heat of reaction is positive. Further investigated parameters, for example the volume of the coolant loop, also affect the freeze start ability, but it can be concluded that the shut down strategy is of main importance.

1. Introduction

The integration of a fuel cell system in a vehicle can be a clean and efficient solution for future mobility. Even if the technology has made a lot of progress during the last years, especially regarding durability and power density, there are still some research-challenges to be met before a fuel cell car will be an adequate alternative to a conventional car driven by an internal combustion engine. Among other duties like, e.g. the reduction of costs, the start and operation ability of fuel cell vehicles needs to be comparable to the state of the art of nowadays vehicles. Regarding low temperatures, this means that a safe freeze start should be possible down to −30 °C. The Department of Energy (DOE) proclaimed as one aim for the year 2010 that a start up of a fuel cell vehicle from −20 °C should be possible within 30 s and by using less than 5 MJ of additional energy [1]. They defined a successful freeze start when 90% of the rated stack power is reached. In the following 50% of the maximum stack power, declared as P_{50}, is used as indicator for a successful freeze start, since that value can often be found in the sector of automotive fuel cell application [2,3]. The freeze start interval τ_{50} between start of power output and P_{50} is a convenient value to compare the quality of different freeze start strategies.

During the last years the freeze start of fuel cells has often been a topic discussed in research and literature. One main characteristic of fuel cells is the fact that they produce, besides electricity and heat, only water as exhaust. At conditions below 0 °C this water forming ice can negatively influence the power output of the fuel cell stack. As soon as the fuel cell operates, water is formed according to the electrochemical reaction. The amount of water directly depends on the current and consequently on the power output of the fuel cell. When residual or produced water freezes inside a fuel cell stack, this can lead to irreversible damage to the cell components, e.g. delamination of the Membrane Electrode Assembly (MEA) or structural breaks in the Gas Diffusion Layer (GDL). Cho et al. [4,5], Hou et al. [6,7] and Kim et al. [8,9] have investigated the influence of residual water in fuel cells by freeze/thaw-cycles. Cho et al. [4,5] found that cycling between −10 and 80 °C leads to 2.3% degradation if water is not purged from the fuel cell before freezing. At the

* Corresponding author. Tel.: +49 5361 940309; fax: +49 5361 95740309.
E-mail address: eva.schiesswohl@volkswagen.de (E. Schießwohl).

0378-7753/$ – see front matter © 2008 Elsevier B.V. All rights reserved.
doi:10.1016/j.jpowsour.2008.11.130

experiments of Hou et al. [6,7] the fuel cells did not show any performance losses after 20 freeze/thaw-cycles between −20 and 60 °C. The cells were purged before freezing with gases containing 58% relative humidity at 25 °C which was probably the reason for the good results. Kim et al. [8,9] investigated in detail the physical degradation of four different MEAs undergoing 30 freeze/thaw-cycles between −40 and 70 °C. The Scanning Electron Microscopy (SEM) images showed delamination of the catalytic layer especially in the areas of the gas channels. They found that thinner membranes lead to less degradation due to ice formation, but even with the best material configurations damages occur. Therefore they propose to remove liquid water from the catalyst layer at shut down prior to freeze start.

Ishikawa et al. [10,11] worked on the analysis of the water produced by power generation at temperatures below the freezing point. For the experiments a single cell with a reactive area of 13 cm^2 was used. The water and ice formation was observed at start up from −10 °C with operation at 0.5 V. They found that if there is no residual ice on the GDL, the water can be produced in a so-called super-cooled state and can maintain this state up to 200 s. This leads to an increase of the current density up to the point of ice formation. In comparison they showed the behavior of the water if the cell was not purge before and ice exists on the GDL even before the freeze start. In that case super-cooled water did not appear and ice grew at the interface between MEA and GDL. The current density broke down nearly immediately after start up.

Yan et al. [12] carried out freeze start experiments under different conditions at a temperature variation from −5 to −15 °C. A successful start was possible at −5 °C if the cell was insulated and pre-purged. At −10 °C air stoichiometry and gas temperature were additionally increased, at −15 °C freeze start was not successful anymore.

Tajiri et al. [13] worked on the effect of current density, purge rate and membrane thickness to the freeze start ability of a single cell with 25 cm^2 reactive surface. They found the duration of purge before freeze start to be a very influencing parameter.

In addition to the irreversible degradation of cell components, the ice built especially on the cathode catalyst layer reduces significantly the reactive surface and therefore inhibits the electrochemical reaction [14]. Furthermore Pinton et al. [15] found that due to the ice formation the electrical resistance of the fuel cell increases. All of this can lead to a temporary power loss depending on ambient temperature and fuel cell properties. Since the water production is a main characteristic of the fuel cells operation and cannot be avoided, it has to be handled during a freeze start. In addition to modifications on stack components favoring a good water outflow, purging of the stack with dry gases is necessary at shut down in freezing conditions as well as during start up. Regarding the system architecture, liquid water for humidification has to be avoided, since huge amounts of ice have to be thawed with high energy consumption. Besides the aspect of water handling, the heat generation Q_G and its distribution influences the freeze start ability of a fuel cell system. The more heat is generated during the freeze start, the shorter is the freeze start time τ_{50}. This is also connected to the thermal mass $(mc_p)_{CLG}$ of the fuel cell stack and the cooling circuit as well as to the freeze start temperature T_{Start}. A freeze start can only be successful, if more heat is generated than is necessary for the system to reach 0 °C:

$$Q_G \geq (mc_p)_{CLG}(0\,^\circ\mathrm{C} - T_{Start}) \tag{1.1}$$

Many experimental results regarding the freezing of fuel cells were achieved by investigation of single cells and under isothermal conditions. Only some authors like, e.g. the research group around Oszcipok [16,17] or Bègot et al. [18] work with fuel cell stacks.

The following work tries to simulate real ambient conditions and system behavior in a climatic chamber to achieve more information on how to start a fuel cell vehicle best. In the first step various experiments were carried out to define and investigate the parameters mainly influencing the freeze start ability of a fuel cell system. Since the stack is not freeze-start optimized the absolute freeze start times are not that important, but the differences which can be seen by varying diverse parameters like thermal mass of the cooling circuit or duration of the shut down strategy.

2. Experimental

2.1. Characteristic of the investigated fuel cell system

For the freeze start experiments a low temperature Polymer Electrolyte Membrane (PEM) fuel cell system was used. The integrated stack consists of n_{Cell} = 60 single cells with graphite bipolar plates and has a maximum power of P_{el} = 2.6 kW at an operation temperature of $T_{CLG,in}$ = 60 °C. The stack was not built up especially for the freeze start experiments, but it had been operated in other test series before.

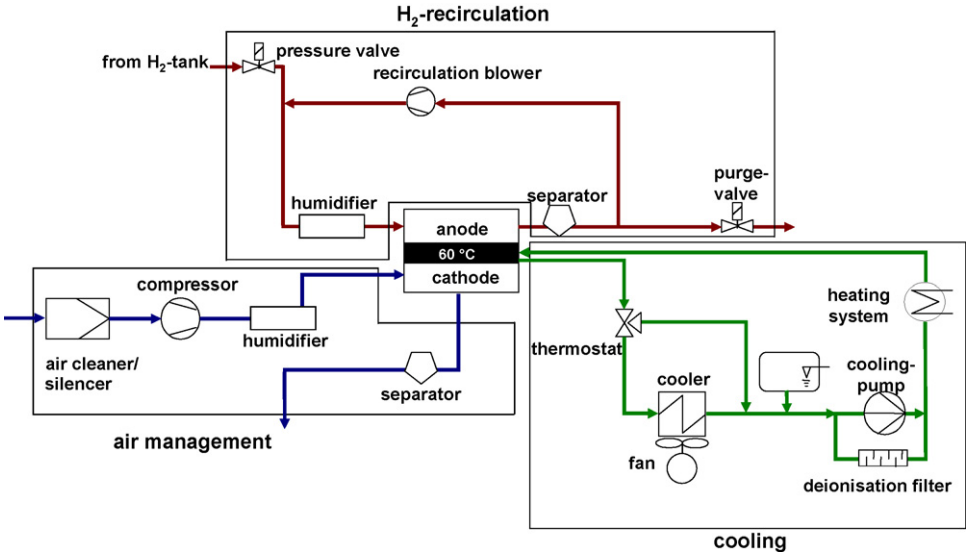

Fig. 1. Investigated fuel cell system.

The fuel cell system (Fig. 1) contains the three main modules: H_2-recirculation, air management and cooling. The gas humidification is realized by contact humidifiers which work by injection and evaporation of liquid water that is separated from the exhaust gases after the fuel cell stack and collected in a water tank. Air is delivered by a compressor and hydrogen through a pressure valve from a high pressure supply.

The cooling circuit contains a mixture of water and ethylene glycol with freezing point at $T_{CLG} = -50\,^{\circ}C$. The cooling fluid flows through the stack, the humidifiers, the air compressor, an additional heater and the deionisation-filter. The heating system is supplementary and was not activated throughout the following freeze start experiments. The cooler is integrated in the circuit via the thermostat. This circuit is the main cooling circuit and in the following it is called "Maxi-Loop". It contains approximately $V_{Maxi} = 4 \times 10^{-3}\,m^3$ of cooling fluid. A smaller "Mini-Loop", which consists only of stack, cooling pump and heating system, is used for the freeze start experiments. Thereby the content of the cooling fluid was reduced to $V_{Mini} = 2.3 \times 10^{-3}\,m^3$ and the thermal mass of the whole loop including the components was reduced to one third of the Maxi-Loops thermal mass. Due to the complex geometry of many components, the thermal mass of the loops was experimentally determined. At room temperature dynamic heating experiments with a constant heat source $\dot{Q}_{in}$ were carried out from $T_{CLG,in} = 20$ to $60\,^{\circ}C$. According to Eq. (2.1):

$$(mc_p)_{CLG} = \frac{\dot{Q}_{in}\Delta t}{\Delta T} \tag{2.1}$$

the thermal mass of the Maxi-Loop was calculated to $(mc_p)_{Maxi} = 65.35\,kJ\,K^{-1}$. For the Mini-Loop the value is $(mc_p)_{Mini} = 22.96\,kJ\,K^{-1}$, whereas the main part of heat, round about 60%, flows into the stack. Since the cooling pump was operated with a constant control signal the volume flow rate varied due to the different pressure drops from $\dot{V}_{Maxi} = 0.45\,m^3\,h^{-1}$ at the Maxi-Loop to $\dot{V}_{Mini} = 0.49\,m^3\,h^{-1}$ at the Mini-Loop.

Various sensors are integrated in all modules to measure temperature and pressure of the fluids between each component. To control the temperature of the stack at three points the temperature of the cooling fluid was measured by thermocouples of the type PT100 (error of measurement ± 0.5%), at the inlet, in the main cooling channel at the entrance of the stack and at the stack outlet. It was decided that the temperature at the stack outlet is most characteristic for the stack temperature, since at this point the cooling fluid is flown through the entire stack.

2.2. Freeze start experiments

The experiments were carried out in a climatic chamber which was conditioned with the investigated freeze start temperature. This does not only affect the ambient and system temperature but also the temperature and condition of the reactant gases. Therefore nearly real ambient conditions could be achieved throughout the experiments. When all components had been stably cooled down to the freeze start temperature, the system was started and the stack was operated with a fixed voltage and without the activation of the heating system. Thereby the power output of the stack was directly affected by the current which corresponds to the start voltage and varies with decreasing of the reactive area in the fuel cell stack through ice formation. The gas flows and pressures were regulated by the control unit of fuel cell system according to the operation point of the stack. After the stack reached P_{50} and the cooling fluid exceeded $T_{CLG,in} = 40\,^{\circ}C$, the start temperature for humidification, the climatic chamber was deactivated and the system was operated at least $t = 30$ min under standard conditions with $T_{CLG,in} = 60\,^{\circ}C$ cooling temperature at the stack inlet, to regenerate the fuel cell stack. Afterwards a polarization curve was measured and then the system was shut down.

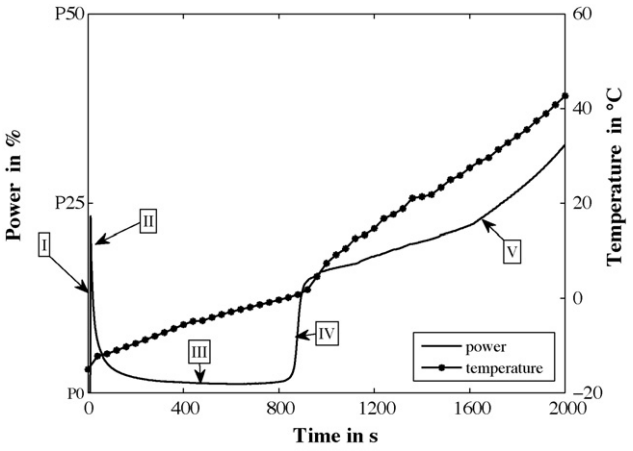

Fig. 2. Typical behavior of power (–) and temperature (*) for freeze starts at low temperatures.

Prior to the freeze start, after the stack and the components had been cooled down to $T_{Sys} = 20\,^{\circ}C$, the system was operated again with a special shut down strategy. The aim of this procedure was the extraction of liquid water from the stack, especially from the cathode side, and the system components which could be damaged through ice formation. In the following the results of two different strategies are presented. The strategy 1 includes the standard operation of the system without external load that means only the components of the system were supplied by the stack power and without gas humidification. The duration of this procedure was $t = 10$ min. During the strategy 2 the system was not started and the compressor was supplied by a battery. The cathode was purged with the same mass flow as during strategy 1 ($\dot{m}_{O_2} = 1.5 \times 10^{-3}\,kg\,s^{-1}$) as long as the relative humidity at the cathode outlet has been fallen below 100%, which was controlled by a humidity sensor as well as by a sight glass. That usually lasts $t = 30$ min. Contemporaneously the anode was purged with dry nitrogen.

2.3. Characteristic freeze start behavior and influencing parameters

At some first test-experiments the system could not be operated in the climatic chamber, therefore a heat input from the environment occurred. Thus it was not possible to use the results for an exact analysis, but, as Fig. 2 shows, the characteristic freeze start behavior of a fuel cell over the entire temperature range could be identified. In literature [12,16,19,20] a description of the first area can be found since that behavior can be usually seen at isothermal freeze starts. The following explanations want to characterize the whole freeze start process up to the nominal operation temperature in a general way.

Regarding the power generation from negative temperatures to the nominal operation temperature five important phases can be identified.

After starting the fuel cell system the voltage is decreased to the fixed value of for example $U_{Cell} = 0.5$ V per single cell. Concurrently the power output increases and also the water production rate (Phase I). If the membrane is saturated and produced water is not extracted from the cell, it will start to freeze and ice blockages will reduce the active cell area (Phase II). This can lead to a strong power loss (Phase III) which lasts until the temperature of the fuel cell stack respectively of the MEA exceeds $0\,^{\circ}C$.

At this point (Phase IV) the ice blockages melt and the gases can reach the reactive area again. Due to the uninhibited reaction, power

Table 1
Summary of the parameters investigated in the following experiments.

Investigated parameters	Variation
Thermal mass, mc_p	Maxi-Loop, Mini-Loop, pump off
Duration of shut down strategy, t	10 min (1), 30 min (2)
Voltage, U_{Cell}	0.45, 0.5, 0.55 and 0.6 V
Temperature, T_{Start}	−6, −8, −10 and −12 °C

increases at first instantly and then according to the influence of flooding processes and of the temperature-dependant conductivity of the membrane (Phase V). It was found that a complete regeneration only takes place close to nominal operation temperature.

This general behavior can be seen at many freeze starts but there are also special cases. For instance, if power and consequently heat generation is too low to reach Phase IV, that means temperature does not exceed the melting point of ice, the reaction will completely break down and a successful freeze start will be impossible. However, on the other hand if the heat generation in Phase I is high enough to avoid ice formation, the power will steadily increase as it is seen in Phase V.

The following experiments investigate this behavior and have the aim to avoid Phase II to IV by finding the right operation conditions. As main influence parameters have been identified the thermal mass (mc_p), which has to be heated up, the duration of the shut down strategy and the start voltage. The thermal mass is varied by reduction of the cooling circuit, from Maxi-Loop to Mini-Loop, and by deactivation of the cooling pump which inhibits heat transfer from the stack to the cooling circuit. The shut down strategy includes a purge of stack and components with dry gases to extract water from the system. The duration and kind of this process were investigated to achieve higher dryness of the stack at freeze start, since that is responsible for the quality of Phase I.

All of these experiments were made at a freeze start temperature of $T_{Start} = -6\,^{\circ}C$, since this was found to be a system specific temperature where stable freeze starts without additional heat source are possible. In addition, further experiments with freeze start temperatures up to $T_{Start} = -12\,^{\circ}C$ were carried out. Table 1 gives a summary of all the variations.

3. Results and discussion

3.1. Reproducibility of the results

Due to practical reasons the fuel cell stack is not operated in a test facility but in a real system. This leads to slightly varying conditions in every experiment. One influencing factor is, e.g. the different amount of liquid or frozen water which is present in the humidifiers during any kind of operation. Variations are approximately in the range of less than 5% of the total water amount. In addition, different system operation between the freeze starts due to not working components which had to be changed or due to other system tests which had to be made can lead to different conditions of humidity in the stack before shut down. Furthermore especially the shutdown strategy 1 did not lead to a reproducible water extraction from the stack as it will be discussed later on. Even if the shutdown strategy 2 leads to much better results, completely identical humidity conditions in every single cell are hardly achievable. In Fig. 3 the distribution of the single cell voltage is shown at a start from $T_{Start} = -6\,^{\circ}C$, with $U_{Cell} = 0.5$ V, Mini-Loop and shut down strategy 1.

The black line indicates the 0.5 V which every cell should have theoretically, but in reality the voltage varies from 0 to 0.8 V. Even if the total voltage of the stack is equal in the experiments, every single cell has a different voltage resulting from differences in water content, state of degradation or gas flowing conditions in the stack.

This behavior was found more or less in the same way during all the freeze starts and therefore it is to assume that it is nevertheless possible to compare the different experiments with each other, since it is compensated over the entire stack.

However, due to that and because of the influence of the whole fuel cell system, identical experiments are unlikely achievable. Furthermore deviations in the freeze temperature of about $\Delta T = \pm 0.5$ K could be possible, since the system was cooled down through air convection in the climatic chamber and even if a fixed temperature was set, the real temperature varied slightly.

Fig. 4 shows the results of two experiments carried out with the shut down strategy 2 and the same conditions ($U_{Cell} = 0.45$ V, $T_{Start} = -6\,^{\circ}C$, Mini-Loop). It can be seen that the general behavior of the fuel cell stack is in both cases the same and after about $t = 60$ s the power differs only slightly. Some deviations occur in the first area which lead, according to the definition for a successful freeze start that means P_{50} is reached, to differences in the freeze start times ($\tau_{50} = 13$ and 49 s). A reason for this could be, asides the influence

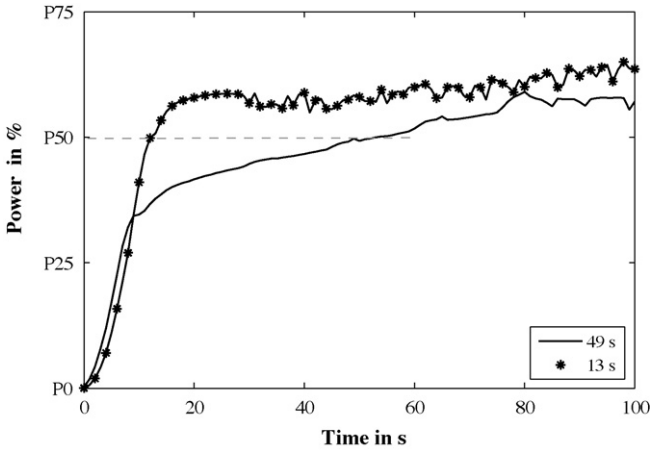

Fig. 4. Time evolution of power for two freeze starts of $\tau_{50} = 13$ s (*) and $\tau_{50} = 49$ s (–) with Mini-Loop at a freeze start temperature of $T_{Start} = -6\,^{\circ}C$, shut down strategy 2 and a start voltage of $U_{Cell} = 0.45$ V.

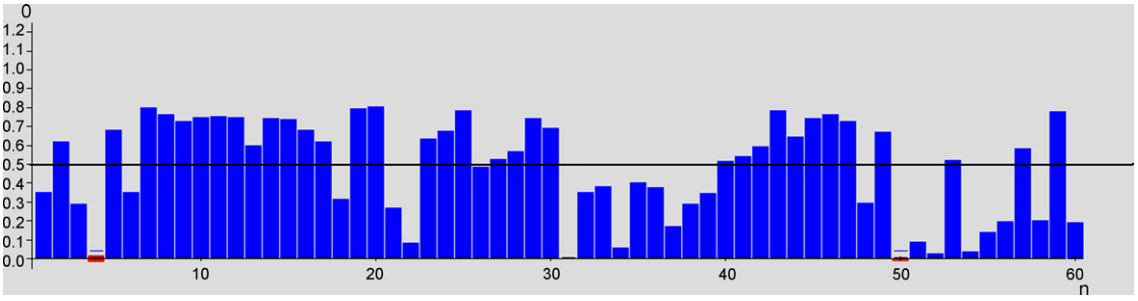

Fig. 3. Distribution of the single cell voltages at a freeze start with $T_{Start} = -6\,^{\circ}C$, $U_{Cell} = 0.5$ V, Mini-Loop and shut down strategy 1.

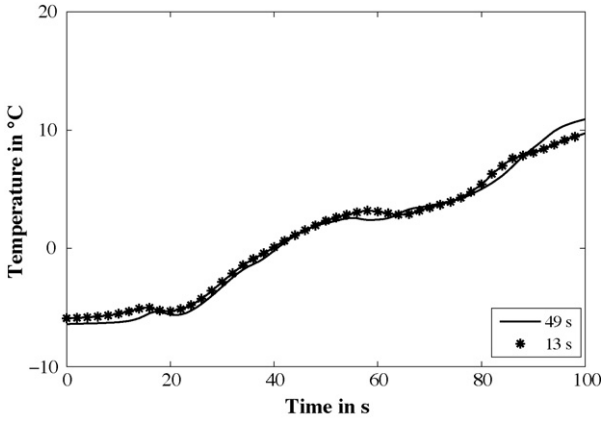

Fig. 5. Time evolution of temperature for two freeze starts of τ_{50} = 13 s (*) and τ_{50} = 49 s (–) with Mini-Loop at a freeze start temperature of T_{Start} = −6 °C, shut down strategy 2 and a start voltage of U_{Cell} = 0.45 V.

from the system, the slightly different cooling temperature which is at the experiment with the faster freeze start ΔT = 0.5 K higher (Fig. 5).

3.2. Reduction of the cooling circuit

One important parameter influencing the freeze start ability of the fuel cell system is the thermal mass. Therefore in the first step the cooling circuit of the investigated system was reduced to the minimum. Via valves all freeze-start irrelevant components were extracted from the cooling circuit. This led to the much smaller cooling circuit Mini-Loop that contains only stack, cooling pump and heater and has at about one third of the thermal mass of the Maxi-Loop, the usual cooling circuit (Fig. 1).

Fig. 6 shows that this reduction influences the freeze start time positively. The increase of stack power is depicted for two freeze starts with the different cooling loops. Both starts are made at a temperature T_{Start} = −6 °C, with shut down strategy 1 and a fixed average voltage of U_{Cell} = 0.45 V. For an improved visualization only every 10th value is marked with symbol.

It is to be expected that by reducing the thermal mass to one third also the freeze start time will be decreased by this factor. However, there are even more factors influencing the freeze start ability and therefore τ_{50} is only reduced from τ_{50} = 690 to 360 s. One reason for this can be seen clearly in Fig. 3. The power peak, that means Phase I, is much higher in the experiment with the Maxi-Loop than in the one with the Mini-Loop. Also Phase III, in which

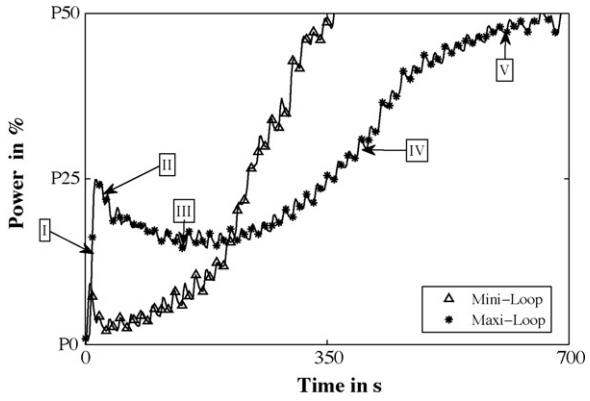

Fig. 6. Time evolution of power for freeze start with Maxi-Loop (*) and Mini-Loop (△) at a freeze start temperature T_{Start} = −6 °C, shut down strategy 1 and a start voltage U_{Cell} = 0.45 V.

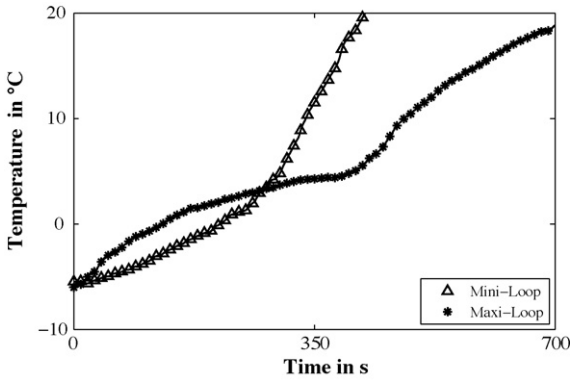

Fig. 7. Time evolution of temperature for freeze start with Maxi-Loop (*) and Mini-Loop (△) at a freeze start temperature T_{Start} = −6 °C, shut down strategy 1 and a start voltage U_{Cell} = 0.45 V.

power output is usually very low, is not really distinctive. During the first period of start this leads to a higher heat production rate than in the experiment with the Mini-Loop and therefore to less ice formation and a τ_{50} which is shorter than expected. The development of the cooling temperature at the stack outlet in Fig. 7 proves that, since at the experiment with the Maxi-Loop the temperature increase more rapidly in the period until 300 s.

Responsible for the quality of Phase I is the water content of the MEA before the freeze start, since this determines the absorption capacity for produced water. If water is neither absorbed nor extracted, it will freeze on the reactive surface of the MEA and reduce consequently the power output as it is seen in Phase II and III. It can be concluded that in the both experiments different conditions of humidity are present in the stack before start up. Therefore further experiments (Section 3.3) discuss the influence of an appropriate shut down strategy to the freeze start ability.

A possibility to improve the freeze start time further is the reduction of heat losses by the deactivation of the cooling pump (Fig. 8). Then only the stack is heated and not the components included in the cooling circuit.

Through this procedure freeze start time was reduced to τ_{50} = 210 s. Since this leads to inhomogeneous temperature profiles and possibly also to hot spots in the stack, only one experiment was made to investigate the effect on the freeze start time.

In that case stack temperature was controlled through the temperature of the air exhaust and the cooling pump was activated when this temperature exceeded $T_{Air,out}$ = 40 °C. Fig. 9 shows the evolution of the temperatures for both experiments at the air outlet

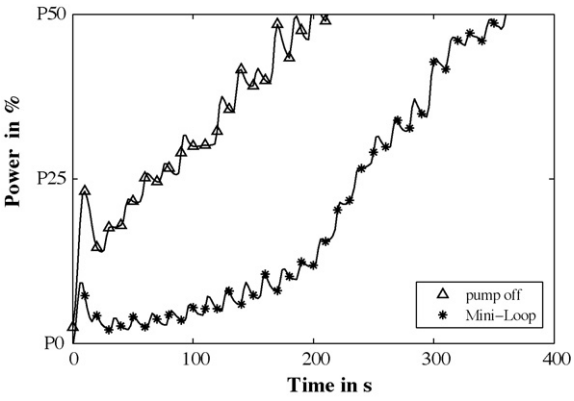

Fig. 8. Time evolution of power for freeze start with Mini-Loop (*) and without activation of the cooling pump (△) at a freeze start temperature T_{Start} = −6 °C, shut down strategy 1 and a start voltage U_{Cell} = 0.45 V.

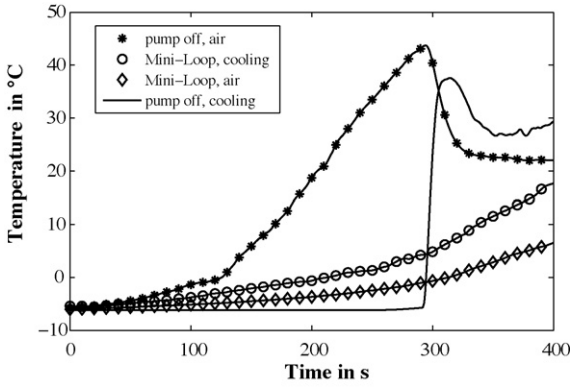

Fig. 9. Time evolution of cooling temperature for freeze start with Mini-Loop (◯) and without activation of the cooling pump (–) at a freeze start temperature $T_{Start} = -6\,^{\circ}C$, shut down strategy 1 and a start voltage $U_{Cell} = 0.45\,V$ as well as time evolution of the air exhaust temperature for Mini-Loop (◊) and without activation of the cooling pump (*).

as well as at the cooling outlet. When the cooling pump is activated the heat is mostly dissipated via the cooling fluid, thus its temperature (◯) is higher than the air temperature (◊). Without a circulation of the cooling fluid the reaction heat is only conducted from the stack by the gas flows. That leads to a fast increase of the temperature (*) at the stack exhaust, especially above $T_{Air,out} = 0\,^{\circ}C$, as it is depicted in the diagram. After approximately $t = 300\,s$ the cooling pump is started and consequently the cooling outlet temperature increases while the air temperature decreases. After a short overshoot the temperature stabilizes at $T_{CLG,out} = 30\,^{\circ}C$ and in the further course it rises according to the stack power.

Throughout these experiments a dependency on the hydrogen purge which is expressed by the oscillating power could be detected. The anode is purged every 15 s to extract water and inert gases from the stack. This improved flow and connected with it the increase of the hydrogen partial pressure seems to have a high impact under these operation conditions.

3.3. Analysis of the shut down strategy

Because of the strong differences regarding the power peak at the beginning of the freeze start, the shut down strategy was analyzed. The shut down strategy of the experiments investigating the influence of the thermal mass included a blowing out of the stack and other critical components with dry gases when the system was cooled down to room temperature, approximately $T_{Sys} = 20\,^{\circ}C$. The blowing out time was $t = 10\,min$ and the stack was operated in this period to provide electrical power to the compressor and other components. In Fig. 10a the photograph shows the water content at the cathode exhaust after this procedure.

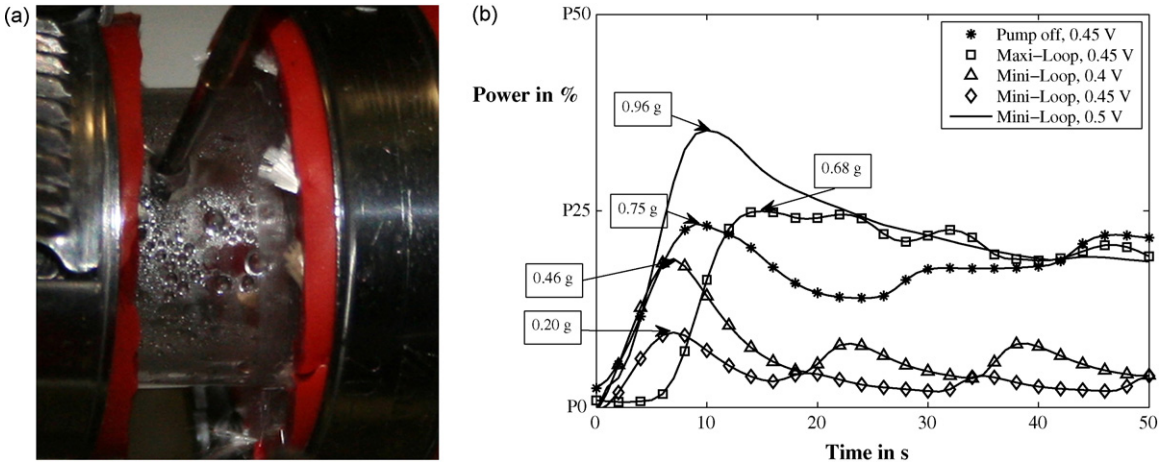

Fig. 10. (a) Photographs of cathode exhaust with shut down strategy 1 and (b) power peaks of different freeze starts at $T_{Start} = -6\,^{\circ}C$ with shut down strategy 1 including the amount of water produced until this peak (Mini-Loop, $U_{Cell} = 0.5\,V$ (–); Maxi-Loop, $U_{Cell} = 0.45\,V$ (□); Pump off, $U_{Cell} = 0.45\,V$ (*); Mini-Loop, $U_{Cell} = 0.4\,V$ (△); Mini-Loop $U_{Cell} = 0.45\,V$ (◊)).

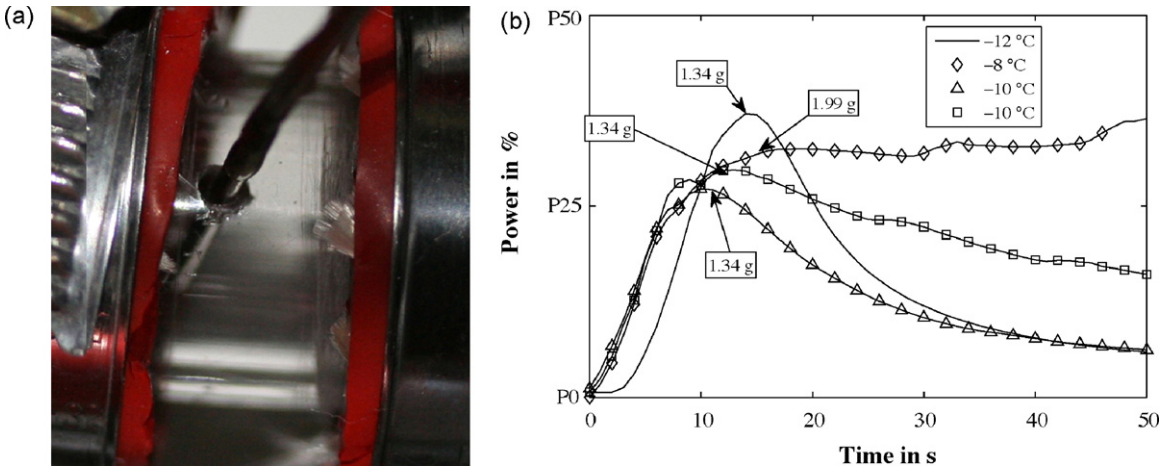

Fig. 11. (a) Photographs of cathode exhaust with shut down strategy 2 and (b) power peaks of different freeze starts with shut down strategy 2, $U_{Cell} = 0.45\,V$ and Mini-Loop including the amount of water produced until this peak ($T_{Start} = -8\,^{\circ}C$ (◊); $T_{Start} = -10\,^{\circ}C$ (□, △); $T_{Start} = -12\,^{\circ}C$ (–)).

Water droplets at the wall are still visible. An investigation of the Phase I at diverse freeze start experiments and the calculation of the amount of produced water up to the power peak show a high level of deviation (Fig. 10b). Besides the experiments discussed in Section 3.2, further experiments with a variation of voltage were carried out. They did not lead to the expected results, because the higher voltage of $U_{Cell} = 0.5\,V$ (–) showed a higher power output than the lower voltage of $U_{Cell} = 0.45\,V$ (◊). In addition, the amount of water which was taken up before freezing varied between $m_{H_2O} = 0.20$ and $0.96\,g$ that corresponds to a factor of 5. Consequently for comparison of different freeze start conditions the shut down strategy 1 is suitable to only a limited extent.

Even if it cannot be the solution to integrate in a fuel cell car, the blowing out time was increased strongly and the components were provided by the battery with the aim to achieve reproducible power peaks. By purging the cathode with dry air and the anode with dry nitrogen for about $t = 30\,min$ a high degree of dryness was visible at the stack exhaust (Fig. 11a). Regarding the power peaks and the amount of produced water before ice formation uniform behavior could be noticed (Fig. 11b). The experiment were made under different conditions of temperature, therefore at the experiment at $T_{Start} = -8\,°C$ no power loss occurred, hence the calculation of $m_{H_2O} = 1.99\,g$ is only a lead. The other three curves have similar power peaks which are in the range of P_{25}. The amounts of produced water are between $m_{H_2O} = 1.01$ and $1.43\,g$ and indicate a higher degree of dryness in the stack respect to strategy 1.

The effect of this improved shut down strategy on the freeze start was found to be enormous. The start time was reduced from $\tau_{50} = 360$ to 13 s. Fig. 12 shows the steady power increase in case of $t = 30\,min$ purge before shut down in comparison with an experiment made with shut down strategy 1 under the same conditions. No power loss is visible and therefore no different freeze start phases. After a short delay due the heat transfer the temperature increases fast and steadily (Fig. 13).

A comparison between Figs. 12 and 13 indicates very well that at about $t = 200\,s$, when the temperature of the experiment with strategy 2 reaches 0 °C, the power increases rapidly. That is the typical behavior of Phase IV as it is described in Section 2.3.

Because of these positive results further experiments were made using the strategy 2 before shut down.

3.4. Variation of the voltage

Another parameter influencing the stack behavior during freeze start is the start voltage. Lower voltage leads to higher current density and consequently to a higher water production rate, but

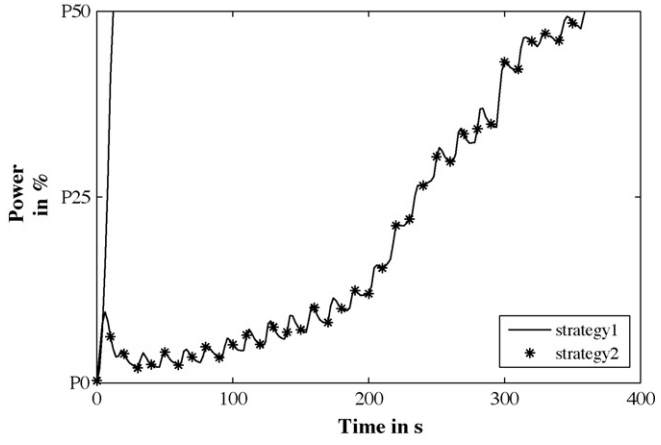

Fig. 12. Time evolution of power for freeze start with shut strategy 1 (*) and strategy 2 (–) at a freeze start temperature $T_{Start} = -6\,°C$ and a start voltage $U_{Cell} = 0.45\,V$.

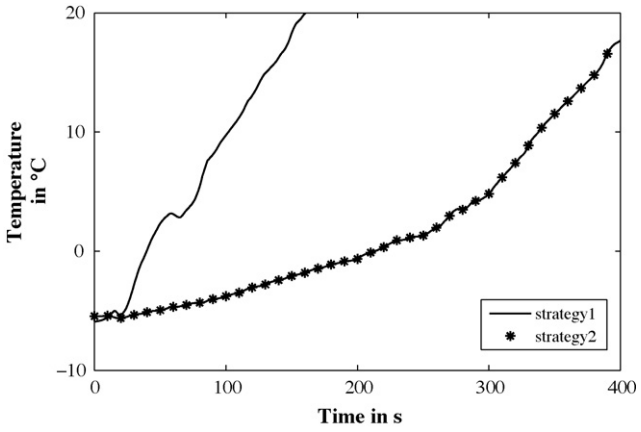

Fig. 13. Time evolution of temperature for freeze start with shut down strategy 1 (*) and strategy 2 (–) at a freeze start temperature $T_{Start} = -6\,°C$ and a start voltage $U_{Cell} = 0.45\,V$.

concurrently also to increased heat generation. The amount of produced water can be calculated by the current per single cell which is defined as

$$I = \dot{n}_{el} F, \tag{3.1}$$

with $F = eN_A = 96.487\,C\,mol^{-1}$ and $\dot{n}_{el} = \dot{n}_{H_2O} n_{el}$ with $n_{el} = 2$ as amount of electrons involved in the reaction.

With the molar mass of water $M_{H_2O} = 18\,g\,mol^{-1}$ and the amount of single cells $n_{Cell} = 60$ the mass flow of produced water can be calculated in every point of operation:

$$\dot{m}_{H_2O} = \frac{I M_{H_2O}}{F \dot{n}_{el}} n_{Cell} \tag{3.2}$$

$$\dot{m}_{H_2O} = 9,33 \times 10^{-5} \frac{g}{C} n_{Cell} I \tag{3.3}$$

The reaction heat of a fuel cell is the difference between the theoretical possible power P_{el} calculated by the thermoneutral voltage U_{th}, in that case for liquid water, and the effective electric power P_{el} depending on the operation point with the voltage U and the current I.

$$Q_G = P_{th} - P_{el} = \frac{U_{th} - U_{Cell}}{I} n_{Cell} \tag{3.4}$$

with $U_{th} = 1.48\,V$.

Table 2 gives an overview of the amount of water produced per second as well as heat generated per second at P_{50} over a range of voltage from 0.6 to 0.45 V. The influence expressed in percent shows, based on the start value at 0.6 V, that heat production increases faster than water generation.

This theoretical estimation could be proved by the experimental results which are summarized in Fig. 14.

The increase of power is depicted for four different freeze starts at $T_{Start} = -6\,°C$, with shut down strategy 2 that means $t = 30\,min$ of purge and variation of voltage. At the nominal operation voltage of $U_{Cell} = 0.6\,V$ the freeze start time τ_{50} is with 400 s the longest. By reducing the voltage with steps of 0.05 V down to $U_{Cell} = 0.45\,V$ the interval τ_{50} is shortened to 230, 85 and 49 s. Besides this it can be seen that only in the experiment with $U_{Cell} = 0.55\,V$ marginal power

Table 2
Influence of voltage to water production and heat generation.

Voltage, U_{Cell}	Produced water m_{mo} at P_{50}	Generated heat Q_G at P_{50}
0.6 V	0.20 g s^{-1} (100%)	1.91 kW (100%)
0.55 V	0.22 g s^{-1} (109%)	2.20 kW (115%)
0.5 V	0.24 g s^{-1} (120%)	2.55 kW (134%)
0.45 V	0.27 g s^{-1} (133%)	2.97 kW (156%)

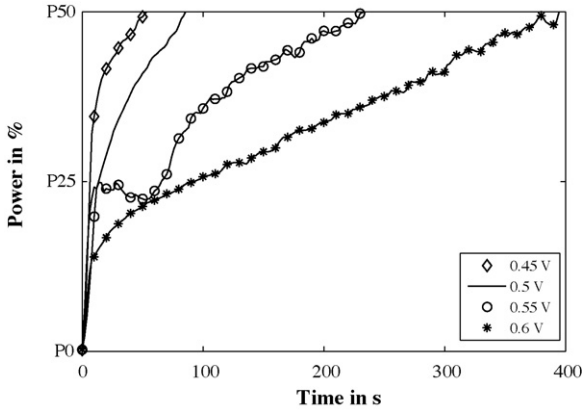

Fig. 14. Time evolution of power for freeze start with shut down strategy 2 at a freeze start temperature $T_{Start} = -6\,^{\circ}C$ and a start voltage of $U_{Cell} = 0.45\,V$ (◊), $U_{Cell} = 0.5\,V$ (–), $U_{Cell} = 0.55\,V$ (○) and $U_{Cell} = 0.6\,V$ (*).

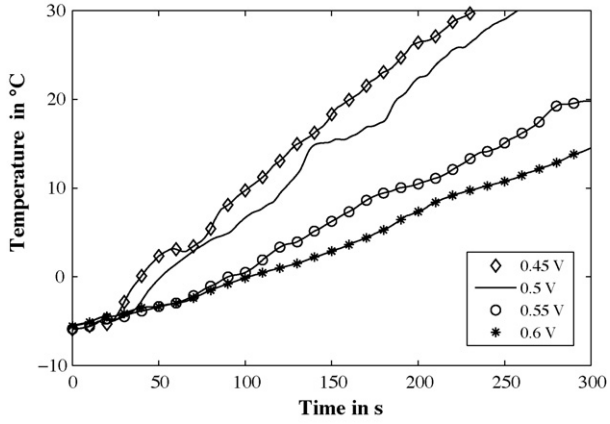

Fig. 15. Time evolution of temperature for freeze start with shut down strategy 2 at a freeze start temperature $T_{Start} = -6\,^{\circ}C$ and a start voltage of $U_{Cell} = 0.45\,V$ (◊), $U_{Cell} = 0.5\,V$ (–), $U_{Cell} = 0.55\,V$ (○) and $U_{Cell} = 0.6\,V$ (*).

loss occurs, in the other cases a stable freeze start proceeds. This is the positive consequence of the higher degree of dryness in the fuel cell stack due to the improved shut down strategy.

Regarding the temperature evolution over time (Fig. 15) in all cases a stable and steady warming up of the system takes place. The velocity of the increase depends on the power output of the stack and is comparable with the results shown in Fig. 14.

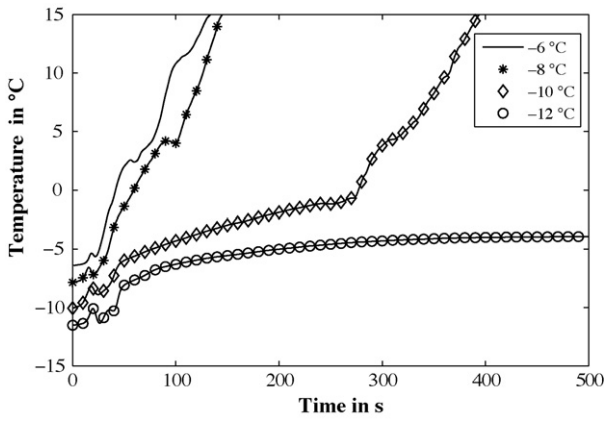

Fig. 17. Time evolution of temperature for freeze start with shut down strategy 2, start voltage of 0.45 V and at freeze start temperatures of $T_{Start} = -6\,^{\circ}C$ (–), $T_{Start} = -8\,^{\circ}C$ (*), $T_{Start} = -10\,^{\circ}C$ (◊) and $T_{Start} = -12\,^{\circ}C$ (○).

3.5. Variation of the freeze start temperature

Considering the previous results, the freeze start temperature was varied with the aim to identify the limit below which successful freeze starts is impossible. Therefore freeze start experiments were made with the best conditions from the former experiment that means with $U_{Cell} = 0.45\,V$, Mini-Loop and shut down strategy 2 to investigate the influence of temperature (Fig. 16). The temperature was reduced from $T_{Start} = -6\,^{\circ}C$ to $T_{Start} = -8$, -10 and $-12\,^{\circ}C$.

It was found that at $T_{Start} = -8\,^{\circ}C$ freeze start time was extended from $\tau_{50} = 13$ to 78 s. Regarding the development of power, no performance loss occurred but for an interval of 20 s the level stays unchanged. In this period probably a kind of equilibrium between water production, ice formation and thawing exists, since the reactive area of the stack is neither reduced nor enlarged. Since power output is already relatively high, temperature increases steadily as it is depicted in Fig. 17. When the stack reaches after ca. $t = 50$ s the temperature of 0 °C, the ice thaws and the power rises more.

At $T_{Start} = -10\,^{\circ}C$ a successful start up is barely possible. Phase III, which indicates the process of ice formation, lasts nearly $t = 3$ min and the entire freeze start time is $\tau_{50} = 460$ s. The temperature evolution in Fig. 17 shows that, even if the power output is with approximately 4 % of the rated power relatively low, heat generation is big enough to let the cooling temperature increase. At about 0 °C, the beginning of Phase IV, in temperature as well as in power evolution a fast increase is visible.

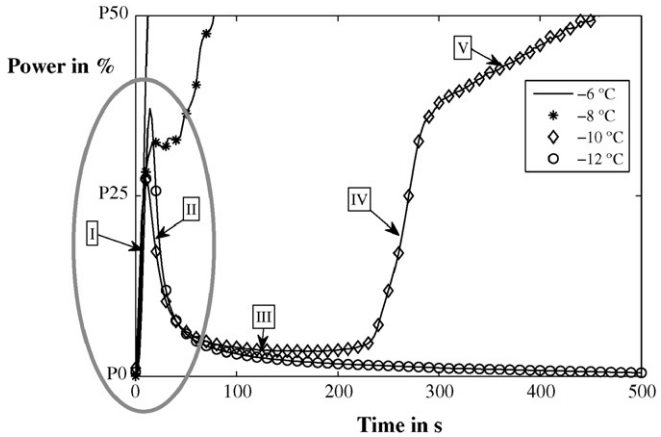

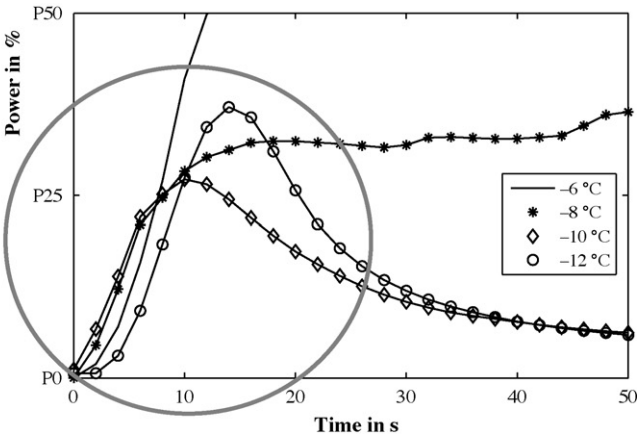

Fig. 16. Time evolution of power for freeze start with shut down strategy 2, start voltage $U_{Cell} = 0.45\,V$ and at freeze start temperatures of $T_{Start} = -6\,^{\circ}C$ (–), $T_{Start} = -8\,^{\circ}C$ (*), $T_{Start} = -10\,^{\circ}C$ (◊) and $T_{Start} = -12\,^{\circ}C$ (○).

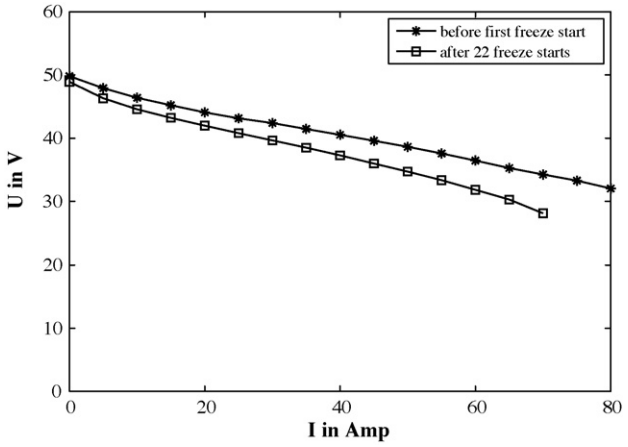

Fig. 18. Polarisation curve before the first freeze start (*) and after 22 freeze starts (□).

In comparison with that, the freeze start experiment of $T_{Start} = -12\,^{\circ}C$ shows what happens if power output is too low to heat up the stack and the surrounded system. After the peak at the beginning of the freeze start, the power does not stay at a constant level in the area between $t = 100$ and 200 s as at the experiment at $T_{Start} = -10\,^{\circ}C$, but it decreases further und further. The continuous growing of ice on the reactive area leads to a complete break down of the reaction. Consequently the temperature does not increase anymore and stays at a level of $T_{CLG,out} = -4\,^{\circ}C$. Under these conditions freeze start is impossible.

3.6. Degradation

As it has already been discussed in the introduction (Section 1), the freezing of residual and produced water can lead to an irreversible damage of the fuel cell components. Furthermore the drying of the MEAs before freeze start might have a negative effect on its durability. Especially regarding stacks it is difficult to realize a homogenous humidity profile in every single cell. Further effort has to be made to find the optimal strategy for that. The way the investigated stack suffered from degradation shows the comparisons of two polarization curves in Fig. 18. At higher loads deterioration up to 18% is visible.

Unfortunately there is no degradation data for the same stack operated at nominal operation conditions available. Therefore it is impossible to distinguish whether the degradation derives from the freeze starts or from conventional ageing processes. Since the stack had already been used in former experiments the influence of ageing is not negligible.

4. Conclusion

The non-isothermal freeze start experiments made with this test system showed that the shut down strategy is the most influential parameter affecting the freeze start time τ_{50}. Preparing the fuel cell before freezing is essentially important for the quality of the following start. For the investigated system a successful freeze start could be realized down to $T_{Start} = -10\,^{\circ}C$ with a maximum freeze start time of $\tau_{50} = 460$ s. It can be concluded that every fuel cell system has a specific freeze start temperature depending on the thermal mass of the fuel cell system, the operation conditions before and at freeze start as well as on the stack characteristics like, e.g. architecture of the flow field or thickness of the membrane. If freeze start is required below that specific temperature, an additional heat source is necessary to support the stack.

Since the shut down strategy includes a purge of $t = 30$ min with dry gases, further investigations have to be made for improving this procedure. Due to the high energy consumption it is unlikely to imagine an integration of that in a fuel cell vehicle. One solution to shorten the purge time at shut down is bypassing the air humidifier of the system, that the water uptake of residual water in the humidifier can be avoided. Besides that, the air mass flow rate can be increased to improve the water extraction from the stack. 2 min are targeted as practical aim for this air purge time.

In addition it was found that thermal mass of the cooling circuit should be reduced to a minimum. Components which do not have to be cooled during start up should be excluded from the cooling circuit like it was done in the investigated system with good success. The deactivation of the cooling pump in the start phase led to improved freeze start times. Since it is not clear yet how this can influence the stack degradation due to inhomogeneous temperature profiles, further experiments have to be made before this can be included in the operation strategy of a fuel cell system.

The theoretical and practical investigation of the stack voltage showed that even if more water is produced, lowering the average voltage below $U_{Cell} = 0.6$ V per single cell leads to more heat generation and shorter freeze start times. Experiments have been made down to average $U_{Cell} = 0.45$ V per single cell, additional experiments are intended. Regarding the integration of that high power operation mode in a fuel vehicle, problems could occur, if the power was not necessary for the power train in the first period after start up. A possible scenario could be that the driver starts the car and stops immediately afterwards, e.g. at the traffic lights. In that case power has to be consumed by internal appliances or loaded in the battery. If that is not sufficient, the voltage will have to be increased according to the required and possible power output.

Therefore further work includes extended test series with a freeze start optimized fuel cell system and stack for vehicle applications. In additions the development of a software tool should support the experiments by theoretical variation of additional parameters.

References

[1] A.A. Pesaran, G.-H. Kim, J.D. Gonder, PEM Fuel Cell Startup Investigation, Milestone Report NREL/MP-540-38760, 2005.
[2] C. Guzy, Fuel Cells for Transportation Application Documentation of the ZEV Technology Symposium, Sacramento, USA, September 25–27, 2006.
[3] T. Brachmann, The Honda Fuel Cell Experience, Documentation of The Fuel Cell, 8th Forum for Producers and User, Stuttgart, Germany, September 29–30, 2008.
[4] E. Cho, J. Ko, Y. Heung, S.-A. Hong, K.-Y. Lee, T.-W. Lim, I.-H. Oh, J. Electrochem. Soc. 150 (2003) 1667–1670.
[5] E. Cho, J. Ko, Y. Heung, S.-A. Hong, K.-Y. Lee, T.-W. Lim, I.-H. Oh, J. Electrochem. Soc. 151 (2004) 661–665.
[6] J. Hou, H. Yu, S. Zhang, S. Sun, H. Wang, B. Yi, P. Ming, J. Power Sources 162 (2006) 513–520.
[7] J. Hou, W. Song, H. Yu, Y. Fu, L. Hao, Z. Shao, B. Yi, J. Power Sources 176 (2008) 118–121.
[8] S. Kim, M.M. Mench, J. Power Sources 174 (2007) 206–220.
[9] S. Kim, B.K. Ahn, M.M. Mench, J. Power Sources 179 (2008) 140–146.
[10] Y. Ishikawa, T. Morita, K. Nakata, K. Yoshida, M. Shiozawa, J. Power Sources 163 (2007) 708–712.
[11] Y. Ishikawa, H. Hamada, M. Uehara, M. Shiozawa, J. Power Sources 179 (2008) 547–552.
[12] Q. Yan, H. Toghiani, Y.-W. Lee, K. Liang, H. Causey, J. Power Sources 160 (2006) 1242–1250.
[13] K. Tajiri, Y. Tabuchi, F. Kagami, S. Takahashi, K. Yoshizawa, C.-Y. Wang, J. Power Sources 165 (2007) 279–286.
[14] S. Ge, C.-Y. Wang, Electrochim. Acta 52 (2007) 4825–4835.
[15] E. Pinton, Y. Fourneron, S. Rossini, L. Antoni, J. Power Sources 186 (2009) 80–88.
[16] M. Oszcipok, M. Zedda, D. Riemann, D. Geckeler, J. Power Sources 154 (2006) 404–411.
[17] R. Alink, D. Gerteisen, M. Oszcipok, J. Power Sources 182 (2008) 175–187.
[18] S. Bégot, F. Harel, J.M. Kauffmann, Fuel Cells 8 (2008) 138–151.
[19] M. Oszcipok, D. Riemann, U. Kronenwett, M. Kreideweis, M. Zedda, J. Power Sources 145 (2005) 407–415.
[20] R. Mukundan, Y.S. Kim, T. Rockward, J.R. Davey, B.S. Pivovar, D.S. Hussey, D.L. Jacobson, M. Arif, R.L. Borup, ECS Trans. 11 (1) (2007) 543–552.